Available online at www.sciencedirect.com

ScienceDirect

Procedia Engineering 213 (2018) 296–302

Procedia Engineering

www.elsevier.com/locate/procedia

7th International Conference on Fatigue Design, Fatigue Design 2017, 29-30 November 2017, Senlis, France

Through Process Modelling applied to the fatigue resistance of cast Aluminum

Yves NADOT[a], Mohamed IBEN HOURIA[a], Raouf FATHALAH[a,b], Daan MAIJER[c]

[a]*Institut Pprime, CNRS, ISAE-ENSMA, Université de Poitiers, Département Physique et Mécanique des Matériaux, Téléport 2, 1 Avenue Clément Ader, BP 40109, F-86961 Futuroscope Chasseneuil Cedex, France*
[b]*LMS, ENIS, BP 264 Erriadh 4023, Sousse, Tunisia*
[c] *Dept. of Materials Engineering, University of British Columbia, Vancouver, BC,Canada V6T 1Z4*

Abstract

The aim of this study is to evaluate a full integrated modelling strategy to evaluate the influence of casting defects on the fatigue life directly from process simulation. We have shown that defects characterized by their size and the microstructure characterized by the SDAS, are the main parameters that control the fatigue limit. A fatigue criterion that already takes into account for the effect of the defect on the fatigue limit was modified to introduce the effect of SDAS. This improved criterion has been employed to predict the Kitagawa diagram for multiaxial loading for different loading cases. The simulation of the modified criterion showed that the reduction of the fatigue limit with the defect size and SDAS is well described. In the last part a numerical model was developed to perform a simulation of the fatigue limit starting from the simulation of the casting process. Using this numerical model, we simulated the defect size and SDAS depending on the solidification time, the fatigue limit is simulated using the improved criterion. We proposed in this part a mold which let to obtain samples with two different microstructures. In this study, a second fatigue tests was carried out on these samples to validate the numerical simulation on the proposed mold. It turns out that the numerical model provides reasonably well the obtained experimental results.

Peer-review under responsibility of the scientific committee of the 7th International Conference on Fatigue Design.

Keywords: Through Process Modelling; Cast Aluminum Alloy; Fatigue design

1877-7058
Peer-review under responsibility of the scientific committee of the 7th International Conference on Fatigue Design.
10.1016/j.proeng.2018.02.030

HCF studies on cast aluminum alloys have shown [1, 2] that the effect of defect size is in competition with other microstructural features such as SDAS/DAS to limit fatigue life. It has been clearly observed that casting defects have a detrimental effect on fatigue limit above a critical size [3, 4]. In addition, the influence of microstructure defined by DAS or SDAS on the fatigue behaviour of cast aluminum alloy cannot be neglected [5-7]. It has been demonstrated [6] that the eutectic phase can cause micro-cracking due to strain accumulation in proximity to Si-particles. As reported in [1], for small defect sizes, there is a prominent interaction between defects and microstructure on the fatigue limit of cast A356-T6 aluminum alloy. Therefore, the simulation of defect size and microstructure distributions within a cast aluminum alloy component are critical inputs for fatigue design. In this context, several studies [8-12] have proposed models to simulate the solidification process and the formation of porosity. A number of models combine the shrinkage pressure and hydrogen concentration to describe porosity formation. In these models the defects were explicitly assumed to be spherical [13-15]. Atwood *et al* [11] assumed that during solidification, due to solid-liquid balance, pore shapes become complex as they grow between grains or between dendrite arms. Several studies [8, 13] have suggested that it is more appropriate to consider an equivalent pore size rather than trying to characterize the complex 3D shape. This assumption is useful in simplifying the fatigue design for casting aluminum alloy components. In some studies [8, 10-12], the effects of pressure, cooling rate and the distribution of hydrogen in the casting on the formation of pores has been studied. Yao et al [8] have shown that the distribution of hydrogen in the liquid phase of the melt depends on the cooling rate, which affects pore growth: the volume of pores decreases when the rate of solidification increases. In the same context, Carlson et *al* [12] developed a model to predict the evolution of porosity during solidification phase. This evolution depends on hydrogen diffusion during solidification. It was shown that, at high cooling rates with a low temperature gradient and low pressure, shrinkage and gas pore formation are more pronounced at low hydrogen concentrations. From this literature summary, the important points that should be considered to predict defect size include the temperature gradient, hydrogen diffusion and local pressure in the melt during solidification. When modeling aluminum alloy casting processes, there are several ways to simulate microstructure formation. Experimental observations have shown that the cooling rate is the major factor that affects dendritic structure [17, 18]. The microstructure of a cast aluminum alloy can be quantified as the SDAS calculated as a function depending on the solidification time or the cooling rate [9, 10, 17, 19]. The aim of the current work is to present a Through Process Modelling for the fatigue design of cast A356 components. This model will be applicable to gravity die cast components. The whole process contains 4 steps: (i) simulation of cooling history during solidification (ii) SDAS simulation based on cooling rate (iii) shrinkage and porosity simulation based on hydrogen diffusion and solidification time, and (iv) fatigue life assessment in a multiaxial context. It is worth noting that the numerical framework developed in this study can be easily extended to any Al-Si-Mg cast aluminum alloy.

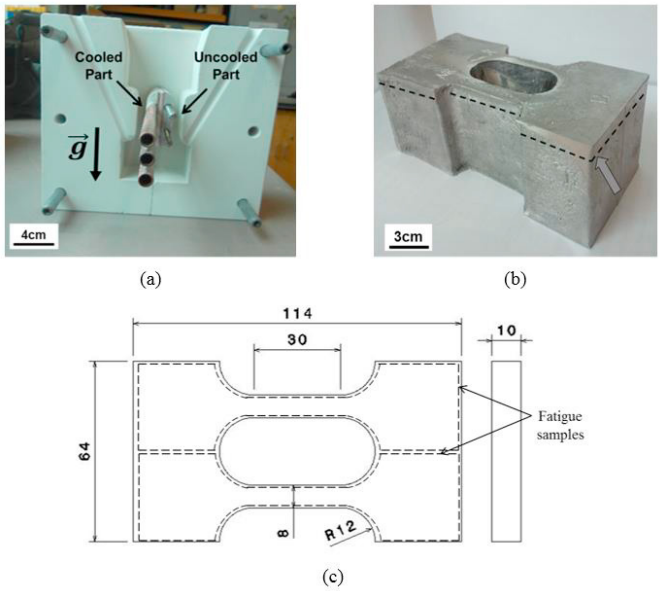

Fig. 1 (a) Mold with cooled/uncooled details (b) resultant casting (c) fatigue specimen geometry

In this study, a purpose built mold was developed in order to vary the SDAS and casting defects with cooling rate and fatigue specimens were extracted from castings produced with the mold. Tension fatigue tests were carried out for two loading ratios: $R_\sigma = 0$ and $R_\sigma = -1$. Finally, a comparison has been carried out between experimental and simulated fatigue limit in order to evaluate the prediction of the Through Process Modelling methodology applied to fatigue design. In previous work [1], it has been shown that defect size and the microstructure described by the SDAS are the main parameters that control the fatigue limit for A356-T6. During solidification, increased cooling rate leads to finer microstructure with less defects. Based on this theory, a mold was designed to vary the cooling rate during the solidification of a casting (Fig. 1). The motivation for developing this mold was to obtain a specified fatigue test specimen geometry with two gauge sections for performing HCF tests (Fig. 1). By creating a cooling rate gradient, the specimens exhibit a varying SDAS and natural defect size. The mold was fabricated from N17, a ceramic material supplied by Foseco. The advantages of using this material were its thermal insulative properties, as well as, the ability to be cut by a water jet cutter. In order to achieve a differential cooling rate on either side of the casting, a central core was fabricated from two copper sections, where one of them was water cooled and the other was solid (refer to Fig. 1). The two copper parts were separated by an insulating paper to avoid heat transfer between the two parts and absorb the contraction during solidification. Fatigue test specimens were then machined from castings produced from this setup. Aluminum alloy A356, without Ar degassing to remove hydrogen, was melted in a resistance furnace and used to fill the mold in this study. The A356 alloy was heated up to 700°C and then poured into the mold under gravity. Before casting, the mold was heated up to 200°C in a separate resistance furnace to remove the humidity. The casting was instrumented with a thermocouple to measure the temperature history during solidification. The results were used to tune the boundary conditions and validate the numerical model. The main mechanical properties for this material for a fine microstructure (SDAS=36µm) are: Young's modulus E=66GPa, Yield stress $R_{p0,2\%}$=164MPa, tensile strength R_m=317MPa and elongation A=16%. Using observations on micrographs taken on polished samples, the SDAS has been determined in the gauges sections of the fatigue specimens taken from the two narrow sections of the casting. As expected, the cooled section exhibits a finer SDAS (29µm) than the uncooled section (75µm; As the cooling rate is the principal parameter that controls dendritic structure in aluminum alloys, this explains the difference in SDAS between the two gauges sections of the fatigue specimens. In order to characterize the defect (pore) size distribution in the casting, a surface analysis was conducted on the two specimens. The size of each pore, quantified using the parameter $\sqrt{area}$, was obtained based on observations from 5 different specimens and then plotted as shown in Fig. 2. The distribution shows that in the cooled section, as expected, the defect size is smaller than in the uncooled section. Using the parameter $\sqrt{area}$ in 2D analyses, the maximum defect size in the cooled section reaches 434µm. On the other hand, in the uncooled section, the maximum defect size reached 579µm. This difference is mainly due to the cooling rate variation within the casting. The variability of the maximum and minimum SDAS and defect size were obtained over the gauge section of the fatigue samples.

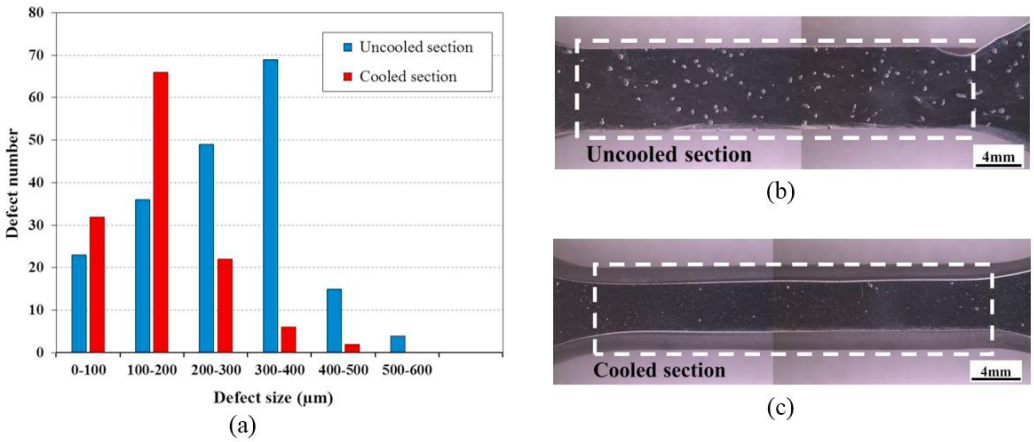

Fig. 2. (a) Experimental defect size distribution in the two different sections (b) uncooled section and (c) cooled section

The fatigue limit simulation was performed for tensile loading with two load ratios: $R_\sigma = 0$ and $R_\sigma = -1$. The fatigue limit prediction was performed using the DSG criterion with Eshelby submodel in a UVARM User-Subroutine for ABAQUS following Mu et *al* [20] work. The fatigue life prediction on the component was performed assuming the material properties for the cast A356 are isotropic and it exhibits linear elastic behaviour with cyclic loading. The 6 components of the local stress tensor on a defect's surface are determined at each point in the domain at times t = 0.25s and 0,75s for cyclic loading with a period t=1s from UVARM subroutine. These two times correspond to the maximum and minimum applied stress during a loading cycle. The deviatoric stress and its variation are calculated to determine the amplitude of the second invariant $J_{2,a}$. The first stress invariant J_1 is identified at these two times t=0.25s and t=0.75s, then the maximum value is considered. The DSG criterion needs both the global stresses far from the defect and the maximum local stress on the defect surface (all details in [1]). This local stress is calculated in the subroutine using the Eshelby's approach [21, 22]. Therefore the maximum Crossland equivalent stress on the defect ($\sigma_{eq\ cr,max}(M)$) and at infinity ($\sigma_{eq,cr}(\infty)$) are obtained. The DSG criterion is given by [1]:

$$\sigma_{eq\ \nabla M} = \sigma_{eq\ Cr,\max} - a_\nabla \frac{\sigma_{eq\ Cr,Max} - \sigma_{eq\ Cr,\infty}}{\sqrt{area}} \leq \beta_0 \exp(-\frac{\lambda_2}{\lambda_0}) \quad (1)$$

Fig; 3 shows the simulated fatigue limit obtained under tensile loading for $R_\sigma = -1$ ratio. The results show that the cooled section has a higher fatigue limit than the uncooled section. This is due to the low defect size and fine SDAS developed in the cooled section.

Fatigue tests under uniaxial tensile loading were performed on specimens extracted from the castings produced for the present investigation containing natural defects. In the case of tensile fatigue tests at $R_\sigma = 0$, the experimental fatigue limit varies between 46 and 48 MPa for sample containing the cooled section and between 38 and 43MPa with the uncooled section. In this case, a quantitative comparison between samples containing the two sections showed a ~ 19% decrease in fatigue limit. Nevertheless, this decrease is more pronounced at $R_\sigma = 0$ (between 55 and 75MPa in the cooled section and between 44 and 67MPa in the uncooled section). The experimental fatigue test results are reported in a Kitagawa diagram [23] for each of the loading cases in Fig. 4. In Fig. 4 with experimental points, the trend of fatigue limit with defect size and SDAS is well described using the DSG criterion. The curve of the DSG criterion is obtained using the average defect size and SDAS in each gauge section. The comparison between predicted and measured results gives a difference of 17% at $R_\sigma = 0$ and 9% at $R_\sigma = -1$. As expected, the DSG criterion predicted reasonably well the interaction between the defect size and the SDAS effects on the fatigue limit.

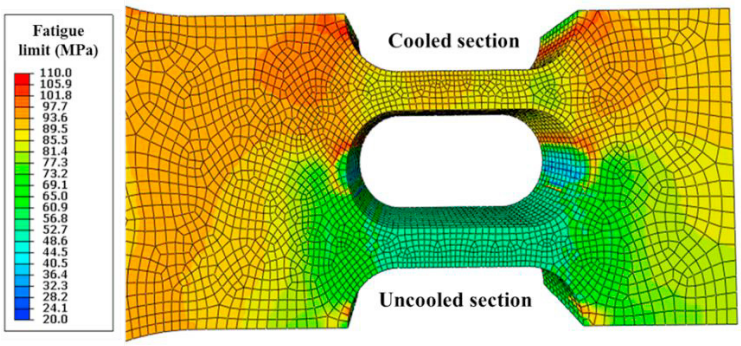

Fig. 3 Simulated fatigue limit in the case of tensile loading at $R_\sigma = -1$

Following the fatigue tests, the defect size observed by SEM in the initiation area varied from 300µm to 750µm in the cooled section and from 500µm to 1000µm in the uncooled section. Referring to Fig. 2, the predicted defect size population presented a maximum defect size of 300µm in the cooled section and 1000µm in the uncooled section. It was shown that the predicted defect size was not representative of the 2D observations made on the surface of the gauge sections. For $R_\sigma = -1$ with defect sizes of 526µm and 589µm in cooled and uncooled sections, respectively, the fatigue limit varies between 76MPa and 67MPa. This difference may be due to two reasons: (i) the interaction between defect size and the SDAS or (ii) the interaction between several close defects as shown in Fig. 5. In the

cooled section, a difference was observed between the measured and the predicted fatigue limit. Based on measured and predicted fatigue limits, a difference was noted in the two gauge sections. It is important to highlight that this difference may be due to the differences between measured and predicted defect size as previously discussed. Fig. 5 presents an SEM image taken of an initiation site on a fracture surface from a sample that failed under tensile loading at R_σ = -1. This specimen was extracted from the cooled section with an measured fatigue limit of 55MPa. In the initiation area, two nearby defects are identified. Both defect sizes (265µm and 354µm) are close to the predicted defect size obtained from the simulation. As the model does not consider possibility of coalescence between defects, this may explain the discrepancy between the measured and the predicted results. Fracture surface observations showed that only surface defects were present at the origin of fatigue failure. These observations confirm that in the case of A356-T6 aluminum alloy under 10^6 cycles fatigue testing, near-surface defects are more harmful than the internal defects. This is consistent with the results of Wang et al [24]. They showed that in the case of cast aluminum alloy A356-T6 for defects located at the free surface, the stress intensity factor is 55% higher than the internal defects.

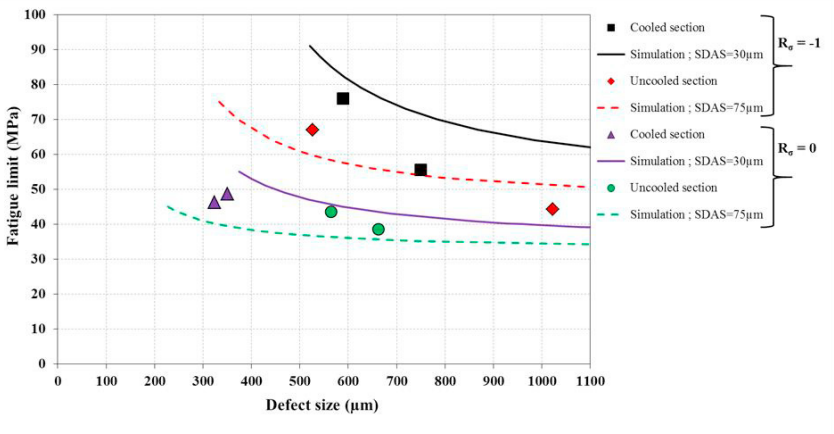

Fig.4. Comparison between experimental results and fatigue limit simulation in a Kitagawa diagram

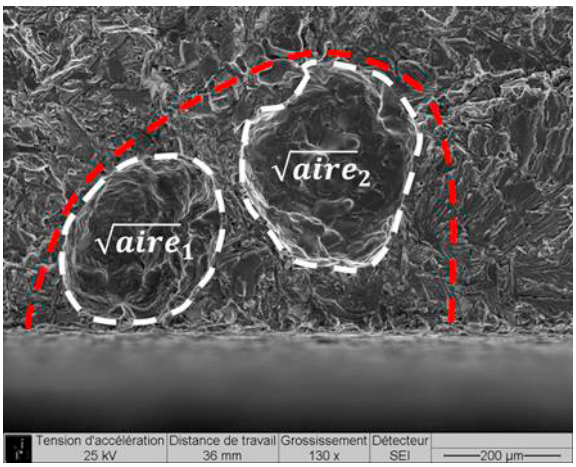

Fig.5. SEM observation of initiation site with two nearby porosities under tensile loading at R_σ = -1 on a cooled specimen ($\sigma_D = 55MPa$, SDAS = 35µm, $\sqrt{area} = 750\mu m$, $\sqrt{area}_1 = 265\mu m$ *et* $\sqrt{area}_2 = 354\mu m$)

Conclusions

The objective of this paper was to predict the fatigue limit of a cast aluminum alloy A356-T6 component starting from a foundry process simulation. A mold was designed to vary the microstructural characteristics of the alloy by

changing the cooling rate in the casting. A Through Process Modeling applied to the fatigue design was presented. The Defect Stress Gradient was used to predict the fatigue limit including SDAS and defect size influence. A comparison between simulation and experimental results was performed. From this study, it may be concluded that:

(i) The model is capable of predicting the evolution of the SDAS in different parts in the casting as a function of the cooling rate. The comparison between measured and predicted SDAS suggests an error of 7%.

(ii) The predicted defect size was accurate overall but better for small defects. The evaluation of defect size distribution from 2D measurements tends to under estimate the real size compared to critical sizes causing failures measured on the fracture surfaces.

(iii) The comparison between measured and predicted fatigue limit using the TPM approach gives an average error of 17% at $R_\sigma = 0$ and 9% at $R_\sigma = -1$.

References:

[1] M. I. Houria, Y. Nadot, R. Fathallah, M. Roy, and D. M. Maijer, "Influence of casting defect and SDAS on the multiaxial fatigue behaviour of A356-T6 alloy including mean stress effect," *International Journal of Fatigue,* vol. 80, pp. 90-102, 2015.
[2] X. Zhu, A. Shyam, J. Jones, H. Mayer, J. Lasecki, and J. Allison, "Effects of microstructure and temperature on fatigue behavior of E319-T7 cast aluminum alloy in very long life cycles," *International Journal of Fatigue,* vol. 28, pp. 1566-1571, 2006.
[3] M. Roy, Y. Nadot, C. Nadot-Martin, P.-G. Bardin, and D. Maijer, "Multiaxial Kitagawa analysis of A356-T6," *International Journal of Fatigue,* vol. 33, pp. 823-832, 2011.
[4] M. Brochu, Y. Verreman, F. Ajersch, and D. Bouchard, "High cycle fatigue strength of permanent mold and rheocast aluminum 357 alloy," *International Journal of Fatigue,* vol. 32, pp. 1233-1242, 2010.
[5] K. S. Chan, "Roles of microstructure in fatigue crack initiation," *International Journal of Fatigue,* vol. 32, pp. 1428-1447, 2010.
[6] Y. Gao, J. Yi, P. Lee, and T. Lindley, "A micro-cell model of the effect of microstructure and defects on fatigue resistance in cast aluminum alloys," *Acta materialia,* vol. 52, pp. 5435-5449, 2004.
[7] L. Ceschini, I. Boromei, A. Morri, S. Seifeddine, and I. L. Svensson, "Microstructure, tensile and fatigue properties of the Al–10% Si–2% Cu alloy with different Fe and Mn content cast under controlled conditions," *Journal of Materials Processing Technology,* vol. 209, pp. 5669-5679, 2009.
[8] L. Yao, S. Cockcroft, J. Zhu, and C. Reilly, "Modeling of Microporosity Size Distribution in Aluminum Alloy A356," *Metallurgical and Materials Transactions A,* vol. 42, pp. 4137-4148, 2011.
[9] J. Guo and M. Samonds, "Modeling of alloy casting solidification," *JOM,* vol. 63, pp. 19-28, 2011.
[10] D. Maijer, Y. Gao, P. Lee, T. Lindley, and T. Fukui, "A through-process model of an a356 brake caliper for fatigue life prediction," *Metallurgical and Materials Transactions A,* vol. 35, pp. 3275-3288, 2004.
[11] R. Atwood and P. Lee, "Simulation of the three-dimensional morphology of solidification porosity in an aluminium–silicon alloy," *Acta materialia,* vol. 51, pp. 5447-5466, 2003.
[12] K. D. Carlson, Z. Lin, and C. Beckermann, "Modeling the effect of finite-rate hydrogen diffusion on porosity formation in aluminum alloys," *Metallurgical and Materials Transactions B,* vol. 38, pp. 541-555, 2007.
[13] P. Lee, A. Chirazi, and D. See, "Modeling microporosity in aluminum–silicon alloys: a review," *Journal of Light Metals,* vol. 1, pp. 15-30, 2001.
[14] D. Poirier, "In Modeling of Casting, Welding and Advanced Solidifi—cation Processes VIII, BG Thomas and C," *Beckermann, eds., TMS, Warrendale, PA,* pp. 837-848, 1998.
[15] K. Kubo and R. D. Pehlke, "Mathematical modeling of porosity formation in solidification," *Metallurgical Transactions B,* vol. 16, pp. 359-366, 1985.
[16] P. Li, P. Lee, D. Maijer, and T. Lindley, "Quantification of the interaction within defect populations on fatigue behavior in an aluminum alloy," *Acta Materialia,* vol. 57, pp. 3539-3548, 2009.
[17] C. Rui, Y.-f. Shi, Q.-y. Xu, and B.-c. Liu, "Effect of cooling rate on solidification parameters and microstructure of Al-7Si-0.3 Mg-0.15 Fe alloy," *Transactions of Nonferrous Metals Society of China,* vol. 24, pp. 1645-1652, 2014.
[18] L. Zhang, Y. Jiang, Z. Ma, S. Shan, Y. Jia, C. Fan*, et al.*, "Effect of cooling rate on solidified microstructure and mechanical properties of aluminium-A356 alloy," *Journal of materials processing technology,* vol. 207, pp. 107-111, 2008.
[19] M. Shabani and A. Mazahery, "Prediction of mechanical properties of cast A356 alloy as a function of microstructure and cooling rate," *Archives of metallurgy and materials,* vol. 56, p. 671, 2011.
[20] P. Mu, Y. Nadot, C. Nadot-Martin, A. Chabod, I. Serrano-Munoz, and C. Verdu, "Influence of casting defects on the fatigue behavior of cast aluminum AS7G06-T6," *International Journal of Fatigue,* vol. 63, pp. 97-109, 2014.
[21] J. Eshelby, "Elastic inclusions and inhomogeneities," *Progress in solid mechanics,* vol. 2, pp. 89-140, 1961.
[22] J. D. Eshelby, "The determination of the elastic field of an ellipsoidal inclusion, and related problems," in *Proceedings of the Royal Society of London A: Mathematical, Physical and Engineering Sciences*, 1957, pp. 376-396.

[23] H. Kitagawa and S. Takahashi, "Applicability of fracture mechanics to very small cracks or the cracks in the early stage," in *Second International Conference on Mechanical Behavior of Materials. ASM, Metals Park, Ohio. 1976, 627-631*, 1976.
[24] Q. Wang, D. Apelian, and D. Lados, "Fatigue behavior of A356-T6 aluminum cast alloys. Part I. Effect of casting defects," *Journal of Light Metals,* vol. 1, pp. 73-84, 2001.